NANO LETTERS

2007
Vol. 7, No. 12
3747−3752

Generation of Molecular-Scale Compositional Gradients in Self-Assembled Monolayers

Pierre Burgos,[†,‡] Mark Geoghegan,[†] and Graham J. Leggett*[,‡]

Department of Physics and Astronomy, University of Sheffield, Hicks Building, Hounsfield Road, Sheffield S3 7RH, United Kingdom, and Department of Chemistry, University of Sheffield, Brook Hill, Sheffield S3 7HF, United Kingdom

Received August 28, 2007; Revised Manuscript Received October 23, 2007

ABSTRACT

Gradients of surface chemical composition were prepared by performing a selective photo-oxidation of self-assembled monolayers (SAMs) of alkanethiols adsorbed on a gold surface, using an ultraviolet laser (244 nm) coupled to an etched optical fiber. In the center of the exposed region, uniform oxidation occurs facilitating uniform replacement of the oxidation products with a second, contrasting thiol, while at the perimeter of the exposed region a gradient of exposure occurs, leading to a gradient of photochemical reaction and, following immersion of the sample in a solution of a contrasting thiol, a gradient of composition. Variation in the exposure is possible by varying the time or the power, and both the height and the width of the resulting gradient may be controlled straightforwardly yielding a simple but highly effective means of generating molecular-scale chemical gradients.

Patterning surfaces to facilitate localized control of the surface energy or composition is a technology of wide-ranging importance with diverse applications including the investigation of biomolecular interactions and the fabrication of microfluidic devices. Microfluidic systems use networks of channels to manipulate small volumes of reagents and are becoming important in diagnostics tools and biological analysis.[1] Surface gradient materials display a continuous change in chemical/physical properties along their length. Microfluidic devices can exploit surface gradients to provide a driving force to induce transport and to provide control of liquid flow. In biology, chemotaxis,[2−4] the process by which cells move up or down a chemical gradient in response to an attractant or repellant, is a major factor in the responses of both bacteria and multicellular organisms to environmental changes. For example, the migration of immune cells through the body during surveillance as well as directed migration toward sites of infection and disease is dependent on chemotactic responses of both antigen-presenting cells and responding cells. Metastatic cells also can use migration to leave primary tumors and colonize target organs. Hence, directional sensing and response play a central role in health and disease. Therefore, an important motivation for the development of methods for fabricating surface gradients is the potential importance of being able to create biomaterial interfaces with tunable properties on small length scales to enable the exploration of interfacial biological phenomena at a fundamental level.

Various methods have been developed to prepare gradient surfaces, relying on vapor-phase diffusion,[5,6] X-rays,[7] photolithography,[8−10] gradual immersion,[11−16] printing,[17,18] photopolymerization,[19,20] photocatalytic methods,[21] and microfluidics combined with photopolymerization.[22,23] Nevertheless, many of these techniques require the use of costly equipment and also significant processing time, both of which present significant drawbacks for their widespread use. Importantly, in addition these methods yield gradients with large length ranges from several micrometers up to millimeters. There is thus a lack of simple, readily implemented methods that are capable of yielding gradients in surface composition on molecular length scales. The present work reports a simple method, which yields gradients in surface chemistry with length scales ranging from the nanometer to the micrometer scale, that is based on the photo-oxidation of a self-assembled monolayer (SAM) of alkanethiols using a UV optical fiber as a source of light.

Alkanethiol molecules adsorb spontaneously onto gold surfaces through the thiol head group forming a SAM. When a hydrophilic (hydrophobic) SAM is irradiated by exposure to light with a wavelength of 244 nm in the presence of oxygen, the alkylthiolate adsorbate complex is converted to a weakly bound alkylsulfonate species in a photochemical reaction, which can be displaced by immersing the sample in a solution of a second, hydrophobic (hydrophilic) thiol.[24−30] In previous work by Leggett and co-workers, the emphasis was placed firmly on the formation of well-defined geometric

* Corresponding author. E-mail: Graham.Leggett@shef.ac.uk.
[†] Department of Physics and Astronomy.
[‡] Department of Chemistry.

10.1021/nl072180h CCC: $37.00
Published on Web 11/14/2007

patterns by spatially selective exposure. There has been no previous demonstration of the use of such a method to form a chemical gradient. In the present study, illumination of SAMs with light with a wavelength of 244 nm and a variable spatial intensity has been examined as a straightforward means of generating a compositional gradient (Figure 1). Importantly, this method enables the imposition of a precisely defined geometric variation in composition, because the composition can be controlled by the selection of the beam profile. A specific beam profile yields an exactly correlative gradient of composition at the sample surface because the extent of photo-oxidation varies with the exposure, and the spatial pattern of exposure reflects the variation in the far-field intensity. After immersion in a solution of a contrasting thiol, oxidized thiolate species are replaced by the second adsorbate yielding a pattern of chemical composition that reflects the UV exposure. Where partial oxidation has occurred as a result of lower levels of exposure, a mixed monolayer will result. As the intensity of illumination varies, following the profile of the beam front, so the composition of this mixed monolayer will vary, yielding a smooth chemical gradient. We illustrate the efficacy of this approach by fabricating a gradient surface with wetting properties continuously changing from hydrophilic (hydrophobic) to hydrophobic (hydrophilic). The height of the gradient and its width may be controlled simply by selecting the diameter of the fiber and the illumination conditions (power and time). In the present study, we have specifically sought to fabricate molecular-scale gradients. However, the method is expected to be readily scaleable (for example, by using a grayscale mask[21] to fabricate larger features).

SAMs were prepared by immersion of chromium-primed gold-coated microscope coverslips in 1 mM solutions of the appropriate thiol in degassed ethanol for at least 24 h. Dodecanethiol (abbreviated $C_{11}CH_3$) and mercaptopropanoic acid (C_2COOH) were purchased from Sigma (Poole, UK). The thickness of the gold film was 25−30 nm. The evaporation rate was kept below 0.2 nm s^{-1}. To facilitate easy location of the micro/nanopattern generated by photo-oxidation, a cross that could be visualized with an optical microscope was drawn on the gold with sharp tweezers.

SAM samples were exposed to UV light with a wavelength of 244 nm from a frequency-doubled argon ion laser (Coherent, Ely, UK) coupled to an optical fiber using a convex lens (Newport, focal length 15 cm). The output power was typically 0.26−0.28 mW. The distance between the laser and the lens was approximately 150 cm. A neutral circular filter (DO = 0−6, Laser Components, Chelmsford, Essex) was used to attenuate the laser power. The optical fiber holder was fixed on a three stage micro-translator (Newport, ULTRAlign Model 561D-XYZ). The diameter of the laser spot was ca. 25 μm in front of the fiber, and the coupling efficiency of the optical setup measured was higher than 90%. A step index multimode fiber (Ceramoptec, Germany) was used, designed specifically to work in the UV range with transmission efficiency higher than 95% at 244 nm for a 5 m length. The numerical aperture was 0.22 ± 0.02. After removing the acrylate jacket by dipping the fiber for 2 min

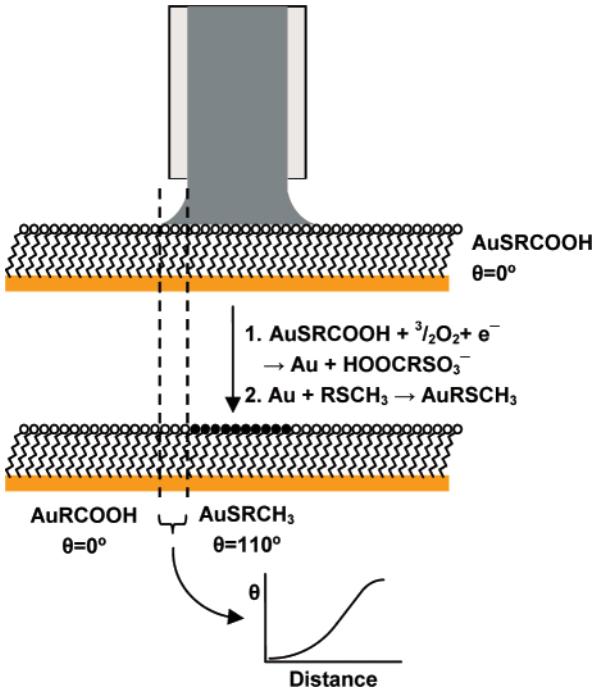

Figure 1. Schematic diagram showing the process used to generate molecular-scale gradients. Exposure of a carboxylic acid-terminated SAM (or a methyl-terminated SAM) to UV light from an optical fiber leads to selective photo-oxidation with a gradient of exposure at the perimeter of the exposed region. Immersion in a solution of a methyl-terminated thiol (or a carboxylic acid-terminated thiol) leads to displacement of the oxidation products and a mixed gradient region with a composition that reflects the gradient of photochemical oxidation.

in dichloromethane, the fiber (of length 1 m) was cleaved to obtain a flat end face. It was then glued to a plastic support and held on a three-axis microtranslator stage or the head of a commercial scanning near-field optical microscope (SNOM; Veeco Aurora III). The distance between the end of the fiber and the gold surface of the sample was maintained at 1 μm or more (far-field optics). Before each experiment, the power emitted by the optical fiber or optical probe was measured with a power meter (Coherent), calibrated at 250 nm.

Friction force microscopy (FFM) was carried out using a Digital Instruments Nanoscope IV Multimode atomic force microscope. The probes used were silicon nitride nanoprobes with a spring constant of 0.06.

Figure 2 shows FFM images of surface chemical gradients fabricated under three different exposure conditions using a fiber with core diameter 50 μm. All images were acquired with the sample under ethanol. In each case, a SAM of C_2COOH was subjected to exposure from the optical fiber and then subsequently immersed in a solution of $C_{11}CH_3$, which displaced the oxidation products formed by the initial exposure and adsorbed at the surface, forming a region of varying composition, which reflected the extent of exposure. The friction force (i.e., the friction contrast) reflected the differences in composition: the material surrounding the exposed area exhibited bright contrast because a comparatively large frictional force was measured for the polar, acid-terminated adsorbate, while the exposed, circular region

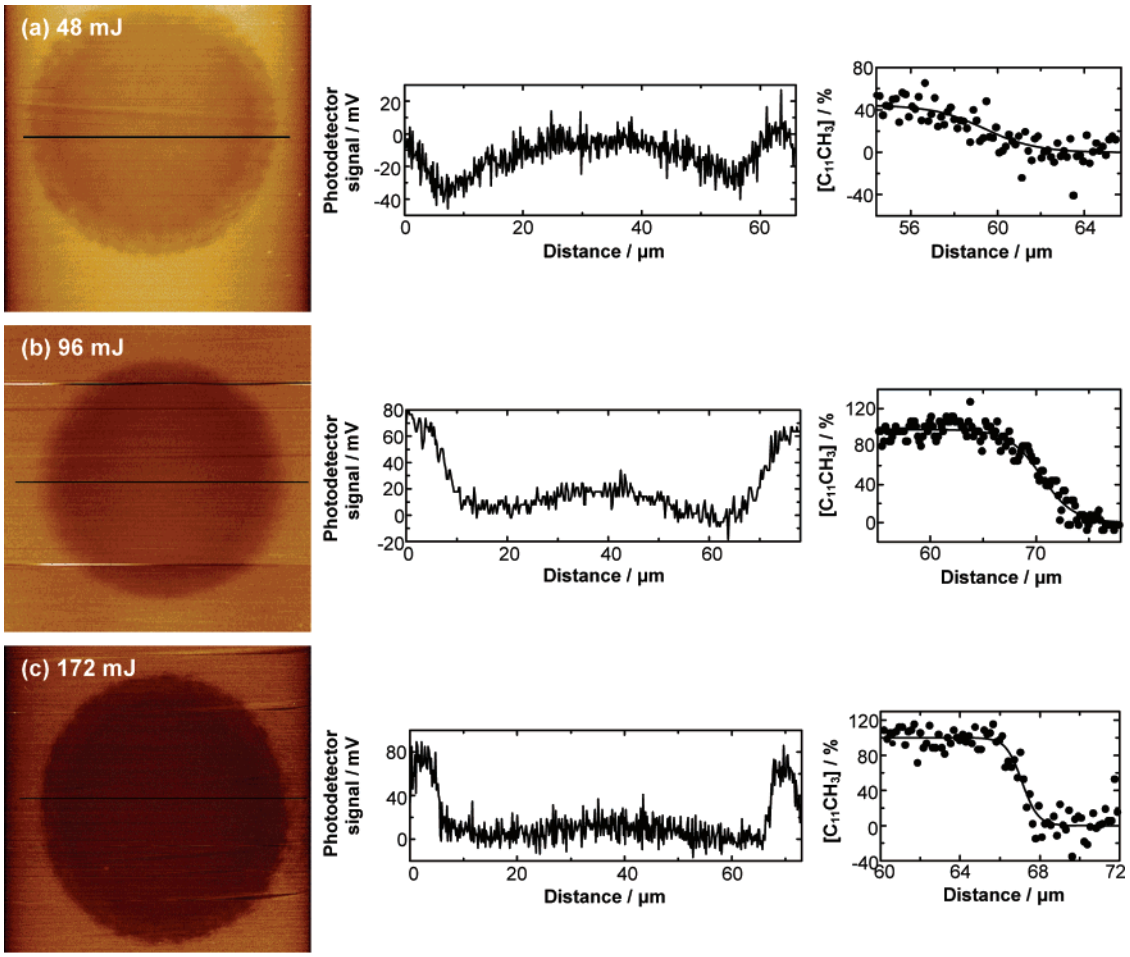

Figure 2. FFM (left) and corresponding friction line-sections (center) for C_2COOH samples subjected to three different exposures and subsequently immersed in a solution of $C_{11}CH_3$. Image sizes: (a) 75 × 75, (b) 82 × 82, and (c) 78 × 78 μm^2. The right-hand figure shows the variation in composition across the gradient region for each specimen. The solid line is in each case a hyperbolic tangent profile with widths (a) 2.4 μm, (b) 3.1 μm, and (c) 800 nm.

exhibited darker contrast because of the partial replacement of the polar adsorbates with nonpolar ones following photo-oxidation. The magnitude of the contrast difference between the central and the exterior regions increased as the extent of exposure increased, reflecting the increasing degree of photo-oxidation. The region around the perimeter of the circular exposed area contained a gradient of composition.

It has been shown previously that there is a correlation between the coefficient of friction and the wettability of the SAM surface. According to Amontons' law

$$F_f = \mu F_N \quad (1)$$

where μ is the coefficient of friction of the area probed, F_N is the load applied normal to the surface, and F_f is the friction force.[31−33] Molecules that differ only in the nature of their terminal groups will yield different friction forces (for example, the coefficient of friction of a carboxylic acid-terminated thiol is ca. twice that of a methyl-terminated one), which facilitates the quantitative mapping of the distribution of surface composition, and hence in the present case enables the surface gradient to be mapped. Measurement of the coefficients of friction of pure $C_{11}CH_3$ and C_2COOH SAMs yielded values of 0.0026 ± 0.0003 and 0.0050 ± 0.0003, respectively. Several areas of 3 μm^2 in the center of each of the three different disk patterns were analyzed. After an exposure of 48 mJ, the coefficient of friction in the central region was 0.0047 ± 0.0003, indicating that it was barely photo-oxidized, and consequently few methyl groups had been introduced. A cross-section through the FFM image showed a correspondingly small difference between the central and external regions with a shallow gradient across the transition region. Careful analysis of Figure 2a suggests that there is in fact a trough around the perimeter of the exposed region where the frictional signal is lowest and that the degree of modification in the center is in fact small. The gradient thus slopes from either side toward a ring that marks the circumference of the central circular area. However, as the exposure increased the coefficient of friction measured for the central, exposed region decreased to 0.003 after an exposure of 96 mJ and to 0.0026 after 172 mJ. After this longer exposure, the coefficient of friction equaled that of $C_{11}CH_3$, and it may be concluded that in the central circular region all of the C_2COOH molecules were oxidized and replaced by $C_{11}CH_3$. The cross-sections support this interpretation.

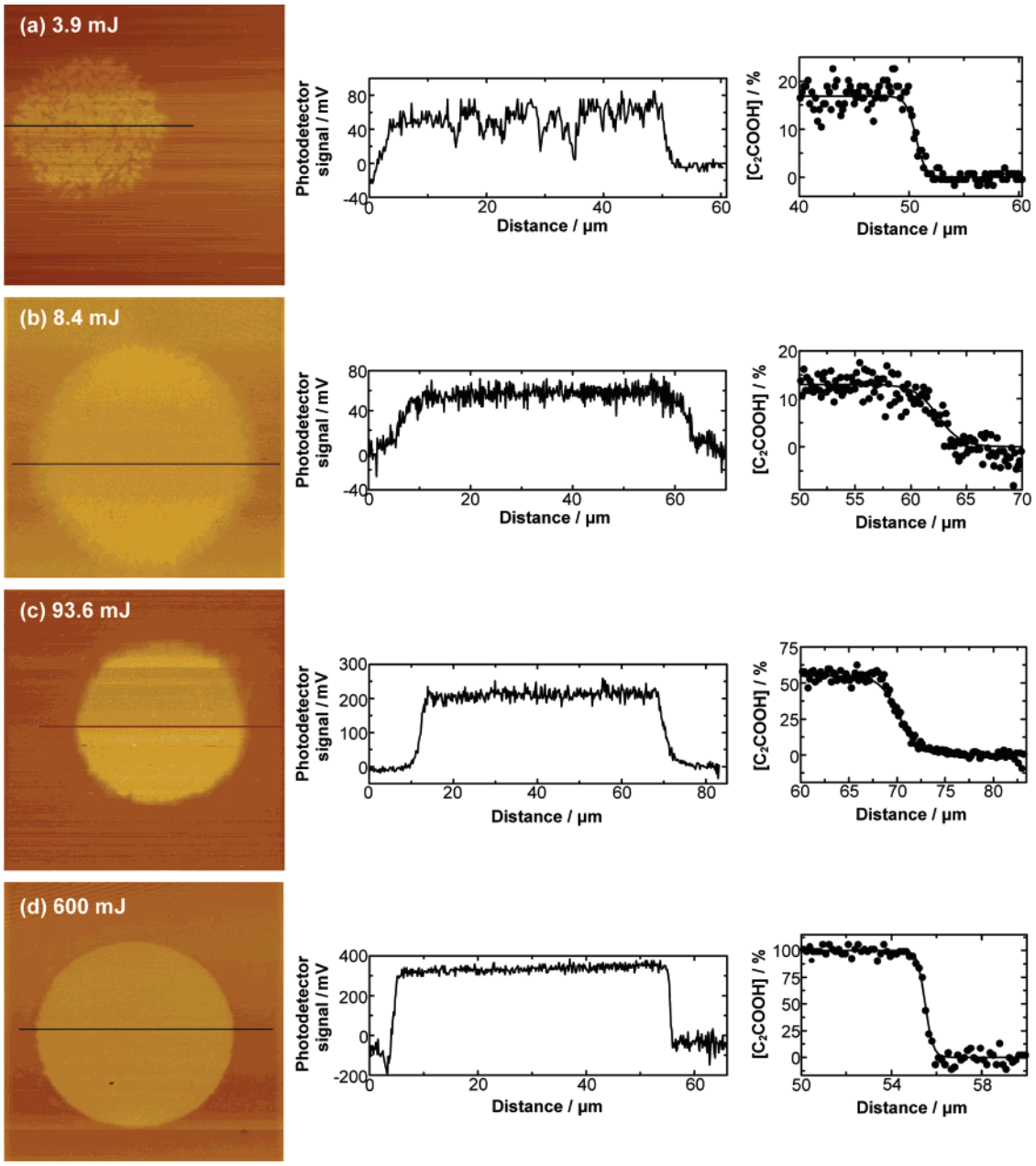

Figure 3. FFM images (left) and corresponding friction line-sections (center) for $C_{11}CH_3$ samples subjected to three different exposures and subsequently immersed in a solution of C_2COOH. Image sizes: (a) 90 × 90, (b) 73 × 73, (c) 97 × 97, and (d) 73 × 73 μm^2. The right-hand figure shows the variation in composition across the gradient region for each specimen. The solid line is in each case a hyperbolic tangent profile with widths (a) 900 nm, (b) 2.1 μm, (c) 2.0 μm, and (d) 340 nm.

The perimeter of the exposed region was analyzed to yield detailed information on the gradients produced. On the basis of the quantitative analysis described above, it is possible to determine the compositional gradient. The composition is expressed in Figure 2 as a percentage of the second thiol ($C_{11}CH_3$ in this case) present at the surface after the second immersion step. It is clear that the height of the gradient increased with exposure as the extent of oxidation in the central circular region increased. The width of the gradient also changed, too. For an exposure of 48 mJ, the gradient was comparatively broad, but as the exposure increased the width of the gradient decreased. In Figure 2a,b, the widths of the gradient were 2.4 and 3.1 μm, respectively, but in Figure 2c, although the extent of oxidation in the central region is similar to that in Figure 2b, the width of the gradient was only 800 nm. These data suggest that not only the height but also the profile of the gradient is controllable simply by controlling the UV exposure.

The process was reversed to prepare a hydrophilic gradient with the same shape. Samples of a $C_{11}CH_3$ monolayer were subjected to a range of exposures at 244 nm and then immersed in a solution of C_2COOH to yield a chemical gradient. The resulting gradients were imaged by FFM (Figure 3). For the shortest exposure, the 50 μm diameter circular region in the center of the exposed area exhibited a patchy appearance, indicating that the oxidation was incomplete and that there was a spatial variation in exposure, leading to a spatially variable incorporation of polar adsor-

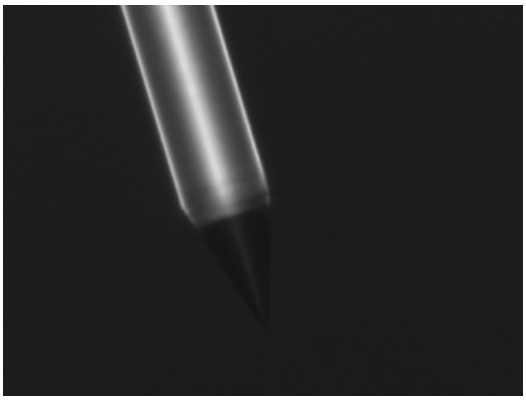

Figure 4. Optical micrograph of an etched probe at the end of a 25 μm diameter fiber.

bates. These observations were attributed to interferences between the propagation modes. In a multimode fiber, there are many possible optical paths (modes) for the light to travel through. Light intensity patterns (the speckle) produced in the output of a multimode optical fiber are complex in nature due first to the launching conditions and second to the interferences of the many modes that propagate down its length. These effects result in an alteration of the complex modal interference pattern at the fiber output. There is a significant random element in the generation of these patterns; any small fluctuation of the laser power or vibration of the fiber will excite fewer or more modes inside the fiber and will create a different speckle pattern.

After a slightly larger exposure (still not sufficient to render the central region more than ca. 15% oxidized), contrast was uniform in the central region, indicating that the effects of laser speckle had become time averaged to a uniform level. The remaining "noise" in the cross-section through the friction image is due to random error in the friction measurement, the largest source of uncertainty in the compositional measurements shown in Figures 2 and 3. As the exposure increased, the contrast difference between the exposed central region and the surrounding material increased with the central region becoming progressively brighter relative to the surrounding material as the extent of oxidation increased. Analysis of the gradient region confirmed that as in the data shown in Figure 2, the width of the gradient region decreased as exposure increased. Initially (Figure 3a) the gradient appears rather sharp, but this is an artificial consequence of the laser speckle that yields localized sharp points. In Figure 2a,b, the width of the gradient was 2.1 and 2.0 μm, respectively, with the width decreasing to 340 nm at the longest exposure.

To facilitate the fabrication of smaller features, optical fibers were etched in a 48% solution (by volume) of HF in water, which is a well-known method for the preparation of nanoprobes for near-field microscopy.[34−36] By adjusting the etching time, we were able to generate small conical structures on the end of the fiber. Etching the fiber for 30 min at room temperature (23 °C) led to the formation of a 5 μm tip at the end of the cleaved fiber (Figure 4). Compared to a cleaved fiber, the electromagnetic field diverges more strongly: the smaller the apex, the wider the angle of diffraction. Therefore, we used a smaller output power during photo-oxidation (<100 μW) and increased the exposure time. A $C_{11}CH_3$ sample, irradiated for 10 min with a 5 μW output power using an etched fiber (power density 9 W cm^{-2}) and immersed in a solution of C_2COOH is shown in Figure 5a. A bright disk of diameter 20 μm was observed and was significantly smaller than the features in Figures 2 and 3. The cross-section shows the formation of a 7 μm wide gradient localized on the edge of the disk. The magnitude of the photodetector signal is larger because the sample was imaged in air. Longer exposures did not enhance the friction contrast, indicating that oxidation was complete after this exposure.

Because in this configuration the diffraction effect was amplified, increasing the distance between the fiber and the

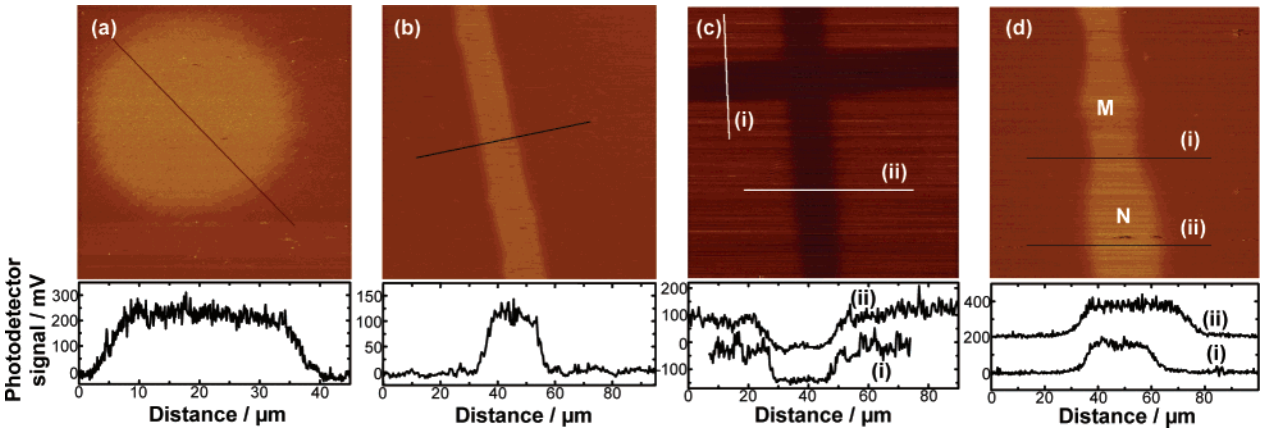

Figure 5. FFM images and corresponding line-sections showing gradients of structures formed by exposure of a sample to light from an etched fiber and immersion in a solution of a contrasting thiol: (a) a spot formed by holding the probe above a $C_{11}CH_3$ monolayer for 10 min with a power of 10 μW, followed by immersion of the sample in a solution of C_2COOH; (b) a line formed by sweeping the probe across the sample during exposure instead; (c) a cross, formed by translating the probe in orthogonal directions across a monolayer of C_2COOH and immersing the sample in a solution of $C_{11}CH_3$; and (d) a more complex structure formed by translating the probe across a $C_{11}CH_3$ surface and then holding it above locations M and N for different periods of time prior to immersion in a solution of C_2COOH to yield gradients of different sizes.

surface yielded a larger spot with a much wider gradient. We were also able to create a variety of other features by simply controlling the motion of the *xy*-microtranslator or the SNOM scan stage. For example, channels were fabricated (Figure 5b) by translating the fiber along a straight line. Control of the speed of translation and the power provided simple but versatile control of the width of the channel and also the height and width of the gradient. Figure 5b shows an FFM image of a $C_{11}CH_3$ sample exposed to an etched fiber scanned back and forth at 10 μm s^{-1} over a period of 15 min with a 45 μW output power and subsequently immersed in a solution of C_2COOH. The linear, exposed region has been oxidized by exposure to the light from the fiber, and the methyl-terminated adsorbates have been replaced by the carboxylic acid-terminated thiol. The channel in Figure 5b has a length of 400 μm and a width of 17 μm. There is a gradient with a width of 4 μm on each side of the channel. Comparison of the contrast in Figure 5a,b suggests that the channel consists of a 1:1 mixture of $C_{11}CH_3$ and C_2COOH, that is, that oxidation is 50% complete.

Figure 5c shows a cross, formed simply by translating the etched fiber in orthogonal directions. Figure 5d demonstrates that highly complex structures may be formed in which gradients with different dimensions are fabricated on adjacent regions of the surface. A gradient channel, like the one in Figure 5b, was fabricated by sweeping the etched probe up and down a hydrophobic sample at a speed of 10 μm s^{-1} with a power of 45 μW. The width of the channel was 16 μm, and the length was 150 μm. At two specific locations, labeled M and N, the probe was held stationary for extended periods of time to create broader gradient structures. Line sections through the original narrow channel and the broad region N, labeled (i) and (ii), respectively, in the figure, demonstrate that in contrast to the behavior observed with the cleaved fiber the etched fiber yields an increase in the gradient width with the time of exposure. The gradient has a (hyperbolic tangent) width of 4 μm when exposed for 4 min and 5 μm when exposed for 11 min, as calculated from the right-hand gradients in Figure 5d.

To summarize, our data demonstrate with good reproducibility that well-defined gradient surfaces with different geometries (dots, channels) may be fabricated on different length scales down to nanometer thicknesses. These features were obtained with different (etched or cleaved) optical fibers. The methodology is readily extendable through the application of other methods for the spatially controlled exposure of SAMs of alkanethiols, too. While we have focused here on the creation of molecular-scale gradients, the same methodology is expected to be applicable on a range of length scales, for example, at the micron scale through the use of a suitable gradient filter. The gradient profile is determined by the input power: high power gives abrupt gradient on the micrometer scale whereas low power generates smoother gradient on a scale of several micrometers; this is valid for all the thiols used whether hydrophobic or hydrophilic. The major advantage of this approach is to engineer a gradient surface with different shapes and profiles easily at a very low cost. Although a commercial SNOM was used for some of these experiments, this is not absolutely necessary; our results simply rely on an optical fiber and a means of scanning this fiber close to the SAM surface.

Acknowledgment. The authors thank the Engineering and Physical Sciences Research Council (EPSRC, Grant GR/T07473/01) for financial support. G.J.L. thanks the EPSRC and the Royal Society of Chemistry Analytical Chemistry Trust Fund for support.

References

(1) Stone, H. A.; Stroock, A. D.; Adjari, A. *Ann. Rev. Fluid Mech.* **2004**, *36*, 381.
(2) Xiao, Z.; Zhang, N.; Murphy, D. B.; Devreotes, P. N. *J. Cell Biol.* **1997**, *139*, 365.
(3) Servant, G.; Weiner, O. D.; Herzmark, P.; Balla, T.; Sedat, W. S.; Bourne, H. R. *Science* **2000**, *287*, 1037.
(4) Ueda, M.; Sako, Y.; Tanaka, T.; Devreotes, P.; Yanagida, T. *Science* **2001**, *294*, 864.
(5) Chaudhury, M. K.; Whitesides, G. M. *Science* **1992**, *256*, 5063, 1539.
(6) Daniel, S.; Chaudhury, M. K.; Chen, J. C. *Science* **2001**, *291*, 633.
(7) Ballav, N.; Shaporenko, A.; Terfort, A.; Zharnikov, M. *Adv. Mater.* **2007**, *19*, 998.
(8) Cao, H.; Tegenfeldt, J. O.; Austin, R.; Chou, S. Y. *Appl. Phys. Lett.* **2002**, *81*, 3058.
(9) Notsu, H.; Kubo, W.; Shitanda, I.; Tatsuma, T. *J. Mater. Chem.* **2005**, *15*, 1523.
(10) Ito, Y.; Heydari, M.; Hashimoto, A.; Konno, T.; Hirasawa, A.; Hori, S.; Kuirta, K.; Nakajima, A. *Langmuir* **2007**, *23*, 1845.
(11) Tomlinson, M. R.; Genzer, J. *Chem. Comm.* **2003**, 1350.
(12) Morgenthaler, S.; Lee, S.; Zurcher, S.; Spencer, N. D. *Langmuir* **2003**, *19*, 10460.
(13) Venkataraman, N. V.; Zurcher, S.; Spencer, N. D. *Langmuir* **2006**, *22*, 4184.
(14) Morgenthaler, S. M.; Lee, S.; Spencer, N. D. *Langmuir* **2006**, *22*, 2706.
(15) Yu, X.; Wang, Z.; Jiang, Y.; Zhang, X. *Langmuir* **2006**, *22*, 4483.
(16) Chang, T.; Rozkiewicz, D. I.; Ravoo, B. J.; Meijer, E. W.; Reinhoudt, D. N. *Nano Lett.* **2007**, *7*, 978.
(17) Kraus, T.; Stutz, R.; Balmer, T. E.; Schmid, H.; Malaquin, L.; Spencer, N. D.; Wolh, H. *Langmuir* **2005**, *21*, 7796.
(18) Choi, S.-H.; Zhang-Newby, B. *Langmuir* **2003**, *19*, 7427.
(19) Harris, B. P.; Kutty, J. K.; Fritz, E. W.; Webb, C. K.; Burg, K. J. L.; Metters, A. T. *Langmuir* **2006**, *22*, 4467.
(20) Harris, B. P.; Metters, A. T. *Macromolecules* **2006**, *39*, 2764.
(21) Blondiaux, N.; Zurcher, S.; Liley, M.; Spencer, N. D. *Langmuir* **2007**, *23*, 3489.
(22) Zaari, N.; Rajagopalan, P.; Kim, S. K.; Engler, A. J.; Wong, J. Y. *Adv. Mater.* **2004**, *16*, 2133.
(23) Burdick, J. A.; Khademhosseini, A.; Langer, R. *Langmuir* **2004**, *20*, 5153.
(24) Brewer, N. J.; Rawsterne, R. E.; Kothari, S.; Leggett, G. J. *J. Am. Chem. Soc.* **2001**, *123*, 4089.
(25) Sun, S.; Leggett, G. J. *Nano Lett.* **2002**, *2*, 1223.
(26) Sun, S.; Chong, K. S. L.; Leggett, G. J. *J. Am. Chem. Soc.* **2002**, *124*, 2414.
(27) Del Campo, A.; Boos, D.; Spiess, H. W.; Jonas, U. *Angew. Chem.* **2005**, *44*, 4707.
(28) Sun, S.; Chong, K. S. L.; Leggett, G. J. *Nanotechnology* **2005**, *16*, 1798.
(29) Brewer, N. J.; Janusz, S. J.; Critchley, K.; Evans, S. D.; Leggett, G. J. *J. Phys. Chem.* **2005**, *109*, 11247.
(30) Leggett, G. J. *Chem. Soc. Rev.* **2006**, *35*, 1150.
(31) Brewer, N. J.; Beake, B. D.; Leggett, G. J. *Langmuir* **2001**, *17*, 1970.
(32) Chong, K. S. L.; Sun, S.; Leggett, G. J. *Langmuir* **2005**, *21*, 3903.
(33) Leggett, G. J. *Phys. Chem. Chem. Phys.* **2005**, *7*, 1107.
(34) Hoffmann, P.; Dutoit, B.; Salathe, R. P. *Ultramicroscopy* **1995**, *61*, 165.
(35) Mononobe, S.; Othsu, M. *J. Lightwave Technol.* **1996**, *14*, 2231.
(36) Puygranier, B. A. F.; Dawson, P. *Ultramicroscopy* **2000**, *85*, 235−248.

NL072180H